THE JOURNAL OF PHYSICAL CHEMISTRY B

Article

pubs.acs.org/JPCB

Phase Diagram of Solvophilic Nanodiscs in a Polymer Solution: Depletion Attraction

Ssu-Wei Hu and Yu-Jane Sheng*

Department of Chemical Engineering, National Taiwan University, Taipei, Taiwan 106, R.O.C.

Heng-Kwong Tsao*

Department of Chemical and Materials Engineering, Department of Physics, National Central University, Jhongli, Taiwan 320, R.O.C.

Supporting Information

ABSTRACT: Entropic attraction between anisotropic nanoparticles in nonadsorbing polymer solutions is significantly greater than that between nanospheres. In this study, depletion attraction between two solvophilic nanodiscs and the aggregation behavior of a nanodisc suspension are explored by dissipative particle dynamics. The depletion force due to polymer addition is proportional to the product of the osmotic pressure and the area of the nanodisc, even for concentrated polymer solutions. For a suspension of nanodiscs, three possible equilibrium states are observed upon polymer addition: dispersion, pretransition, and phase separation. By varying nanodisc concentration (φ_D) and polymer concentration (φ_P), the phase diagram is obtained. Dispersion exists for small φ_D and φ_P. As φ_D exceeds critical aggregation concentration, finite sized clusters are mainly formed with columnar structure in the pretransition regime, similar to micellization associated with typical surfactants. The mean size of columnar clusters seems to grow with $\varphi_D^{1/2}$ and φ_P. For high enough φ_D and φ_P, finite sized clusters vanish and phase separation appears. The nanodisc-rich phase is formed by a bundle of columns or a pack of columns owing to face-to-side and side-to-side depletion attractions.

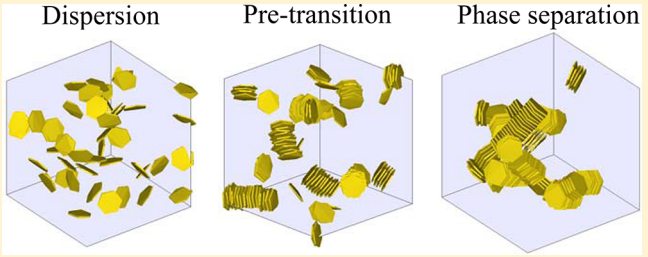

I. INTRODUCTION

For a suspension of colloidal particles in a solvent, the van der Waals attraction causes aggregation of particles, while steric repulsion, electrostatic repulsion, or repulsive hydration force tends to stabilize the dispersion. When the interparticle repulsion dominates over the attraction, a stable colloidal dispersion results. However, nonadsorbing polymers are often added to such a dispersion to drive aggregation[1−3] owing to the modification of the effective interactions between the colloids. This polymer-mediated interaction is referred to as the depletion force, and it was first suggested by Asakura and Oosawa.[4] By this means, phase separation can be induced and thus the isolation of colloids can be facilitated. For example, mixtures of viruses and polymers are widely used for the formation of colloidal liquid crystals.[5] In addition, different sizes and various shapes of Au nanoparticles can be separated through the formation of reversible flocculates by surfactant micelle induced depletion interaction.[6]

The physical origin of the depletion force is that the overlap of the excluded volumes, i.e., depletion zone (V_D), associated with the two nanoparticles increases the volume accessible to polymers and solvents. As a consequence, the entropy of the system is increased ($\Delta S > 0$). Since the internal energy change associated with the contact of two solvophilic nanoparticles is negligible, their free energy decreases due to the contribution $-T\Delta S$. Such an attraction is essentially an entropic force. On the other hand, when the two nanoparticles approach each other, the exclusion of polymers between them leads to a polymer concentration difference between the gap and the bulk. Such a concentration difference results in the osmotic pressure difference (Π), which is described by the van't Hoff equation for a dilute polymer solution. This unbalanced osmotic pressure will push nanoparticles together, and an effective attraction between them is then produced. On the basis of this concept, the depletion potential (A_D) is usually expressed as the product of osmotic pressure and excluded volume, $A_D = \Pi V_D$,[7] for a dilute polymer solution.

The range of the depletion interaction is determined by the size of the polymers (small particles), and its interaction profile depends on the shape of the nanoparticle and the polymer density (ρ_p).[7] For instance, the depletion force between two spheres of radius R surrounded by smaller polymers of radius of gyration r is estimated as $F_D \approx \pi(\rho_p k_B T) rR$ as $R \gg r$. For colloids whose radius is $R = 1$ μm surrounded by polymers with $r = 2$ nm at a concentration $\rho_p = 5$ mM, the depletion force is about $F_D \approx 75$ pN, which is much less than the typical van der

Received: November 27, 2012
Revised: February 24, 2013

   dx.doi.org/10.1021/jp311657q | J. Phys. Chem. B XXXX, XXX, XXX−XXX

Waals force between two spheres, $F_{vdW} \sim 1000$ pN.[8] This consequence indicates that the depletion force is relatively unimportant for spherical nanoparticles because of small R. Moreover, when one regards the solvent molecule as depletant, its contribution to the depletion force between two spheres is also small compared to F_{vdW} because of small r. If one assumes $r = 0.2$ nm and the osmotic pressure is 1 atm, one has $F_D \approx 61$ pN only.

Although the depletion force between spherical colloids is generally weak, it may become quite significant for colloidal discs. On the basis of the force per unit area between two parallel plates, the depletion force between two colloidal discs of radius R can be estimated by $F_D \approx (\rho_p k_B T)\pi R^2$. As a result, for nanodiscs of radius only $R = 45$ nm at a concentration $\rho_p = 5$ mM, a depletion force of about $F_D \approx 75$ pN can be reached. When the disc radius is increased to $R = 160$ nm, the magnitude of F_D becomes comparable to F_{vdW}. It should be noted that the size of the depletant seems to have no influence on the strength of the depletion force but has a major effect on the interaction range.[9] In other words, the depletion force may be significant even in the absence of nonadsorbing polymers and it is caused by the deficiency of the solvent molecules in the overlap region of the depletion layers.

The depletion interaction between spherical colloids has been the focus of decades of study. However, many aspects involved with the entropic interaction between anisotropic particles are still poorly understood. For example, it is known that the strength of depletion interaction is manifested through the characteristic size of nanoparticles. However, how does the size dependence vary with the shape of nanoparticles? Furthermore, for a suspension of nanoparticles, higher polymer concentration is required to exhibit a significant depletion attraction. However, as we know, the van't Hoff equation fails to describe the osmotic pressure in the concentrated regime. Will the relation $A_D = \Pi V_D$ still be valid for high ρ_p? In addition, phase separation or aggregation of nanoparticles is a collective behavior and they are influenced by nanoparticle concentration as well. Therefore, to study the phase behavior driven by depletion attraction, in addition to factors such as the size and shape of nanoparticle and polymer concentration, nanoparticle concentration should also be considered.

In this work, dissipative particle dynamics (DPD) simulations are adopted to explore the depletion interaction between two solvophilic nanodiscs and the aggregation behavior of a nanodiscs suspension. After a brief description of the simulation method and the system, the simulation results are organized as follows. First, the depletion force between nanodiscs is evaluated by computing the effective interparticle interaction via a direct calculation of the force acting on two nanoparticles at a fixed distance. The variation of depletion force with nanodisc size is examined, and the influence of polymer concentration on the depletion force is studied as well. Second, the outcomes of nonadsorbing polymer addition to a suspension of nanodiscs are observed. The dispersion phase and phase separation are identified by observing the variation of mean aggregation number with time. Third, the pretransition phase is seen and finite clusters are formed as the nanodisc concentration exceeds a critical value before phase separation. The mean size of clusters can be controlled by polymer concentration and nanodisc concentration. Finally, the morphological phase diagram is presented.

II. MODEL AND SIMULATION METHOD

The dissipative particle dynamics (DPD) method is a coarse-grained particle based mesoscopic simulation technique that explicitly includes solvents and reproduces hydrodynamic behavior. Introduced by Hoogerbrugge and Koelman in 1992,[10] this method combines some of the detailed description of molecular dynamics (MD) simulations but allows the simulation of hydrodynamic behavior in much larger, complex systems, up to the microsecond range. Like MD, DPD beads obey Newton's equation of motion.[11−13]

$$\frac{d\mathbf{r}_i}{dt} = \mathbf{v}_i, \qquad \frac{d\mathbf{v}_i}{dt} = \frac{\mathbf{f}_i}{m_i} \tag{1}$$

where a bead with mass m_i represents a block or cluster of several atoms or molecules moving together in a coherent fashion and $\mathbf{f}_i$ denotes the total forces acting on particle i.

The interparticle force F_{ij} exerted on bead i by bead j is a sum of a conservative term ($\mathbf{F}_{ij}^C$), a dissipative term ($\mathbf{F}_{ij}^D$), and a random term ($\mathbf{F}_{ij}^R$). Therefore, the total force acting on bead i is given by

$$\mathbf{f}_i = \sum_{j \neq i} (\mathbf{F}_{ij}^C + \mathbf{F}_{ij}^D + \mathbf{F}_{ij}^R) \tag{2}$$

The sum acts over all beads within a cutoff radius $r_c = 1$ beyond which the forces are neglected. Typically, the conservative force is represented by a soft-repulsive interaction

$$\mathbf{F}_{ij}^C = a_{ij}(r_c - r_{ij})\underline{\mathbf{r}}_{ij}, \qquad \text{for } r_{ij} \leq r_c;\ 0, \text{ for } r_{ij} > r_c \tag{3}$$

where r_{ij} is the distance between the two beads and $\underline{\mathbf{r}}_{ij}$ is the unit vector in the direction of the separation. The interaction parameter a_{ij} represents the maximum repulsion between beads i and j. If species i and j are fairly compatible, one has $a_{ij} \approx 25$. As the incompatibility between i and j rises, the value of a_{ij} increases. The dissipative force is proportional to the relative velocity, $\mathbf{F}_{ij}^D = -\gamma\omega^D(\underline{\mathbf{r}}_{ij}\cdot\mathbf{v}_{ij})\underline{\mathbf{r}}_{ij}$, where γ is the friction coefficient and $\mathbf{v}_{ij}$ is the velocity vector of bead i with respect to bead j. The random force is related to the temperature, $\mathbf{F}_{ij}^R = \sigma\omega^R\theta_{ij}\underline{\mathbf{r}}_{ij}$, where $\sigma = (2\gamma k_B T)^{1/2}$ represents the noise amplitude and θ_{ij} is the random number whose average number is zero. The weight functions ω^D and ω^R are r_{ij}-dependent, and we choose $\omega^D = (\omega^R)^2 = (1 - r_{ij}/r_c)^2$ for $r_{ij} \leq r_c$ and 0 otherwise in order to satisfy the fluctuation−dissipation theorem.

In our system, there are three different species of DPD particles, including solvent beads (S), polymer beads (P), which are used to construct a polymer chain, and solvophilic beads (D) for constructing nanodiscs. Typically, the interaction parameter between the same species is set as 25, which yields the compressibility of water as the number density is set as $\rho = 3$. Therefore, one has $a_{SS} = a_{DD} = a_{PP} = 25$. Since the nanoparticle is solvophilic, the repulsive interaction between nanoparticle and solvent is chosen as $a_{DS} = 25$. Similarly, for the nonadsorbing polymer, we have set $a_{PS} = a_{PD} = 25$. It should be noted that the properties and densities of polymer and solvent are the same.

A linear polymer is constructed by connecting L_p DPD beads with springs, and its chain length is characterized by L_p. For instance, there are 12 DPD beads connected together for a chain with $L_p = 12$. In this work, all simulation results are obtained for $L_p = 12$. A nanodisc is constructed by a cluster of DPD beads connected with springs, and the diameter of the nanodisc is much greater than its thickness. Examples of nanodiscs are silver,[14] graphene,[15] zirconium phosphate,[16] and

dx.doi.org/10.1021/jp311657q | J. Phys. Chem. B XXXX, XXX, XXX−XXX

laponite.[17] A nanodisc is modeled with two layers of hexagon, which consists of beads in a hexagonal arrangement.[18,19] The size of the nanodisc is characterized by the diagonal span on the hexagonal face. For example, Dn denotes a nanodisc with the diagonal distance being n DPD beads, and nanodisc D5 is demonstrated in Figure 1. Note that the density of the nanodisc is about 3.8 which is slightly higher than that of solvent.

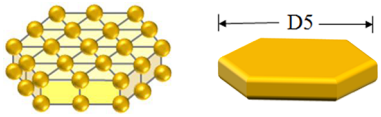

Figure 1. Schematic diagram of the nanodisc with diameter D5.

The adjacent beads in a polymer chain and in a nanoparticle are connected via harmonic spring forces F_{ij}^{S} represented by $\mathbf{F}_{ij}^{S} = -C(r_{ij} - r_{eq})\underline{\mathbf{r}}_{ij}$, where the spring constant is $C = 100$ and r_{eq} denotes the equilibrium length with a typical value of 0.7. The spring force is used to impose connectness among beads in the polymer chain and the nanoparticle, and the choice of C and r_{eq} will not influence the qualitative behavior of the system studied in our work. To further stabilize the structure of a nanoparticle, an additional face diagonal harmonic spring forces[20−22] is adopted. The difference between the two spring forces is the equilibrium length. For the face diagonal spring, the equilibrium length depends on the diameter of nanodiscs (Dn) and can be expressed as $r_{eq} = 0.7(n - 1)$.

On the basis of the algorithm described above, the dynamics of 823 875 DPD beads (N_{tot}) was simulated in a cubic box of length L ($L = 65$) under periodic boundary conditions. The number density of all beads in this system is equal to 3. In DPD simulations, all the units are scaled by the particle mass m, cutoff distance r_c, and thermal energy k_BT. Hence, the length, time, the interaction parameter, and the number density of the system are dimensionalized as $r = r'/r_c$, $t = t'/(mr_c^2/k_BT)^{1/2}$, $a_{ij} = a'_{ij}/(k_BT/r_c^2)$, and $\rho = N_{tot}/(L/r_c)^3$, where x' denotes parameters before scaled. Once all forces are specified, Newton's equation of motion was integrated using the modified velocity-Verlet algorithm with $\lambda = 0.65$. The DPD time step was set at a relatively small value $\Delta t = 0.04$ to avoid divergence of the simulation, and the total DPD steps are at least 8.5×10^5.

The volume fractions of nanodiscs (φ_D) and polymers (φ_P) in the system are defined as

$$\varphi_D = \frac{N_D M_D}{N_{tot}} \tag{4}$$

and

$$\varphi_P = \frac{N_P L_P}{N_{tot}} \tag{5}$$

where N_D and N_p represent the total number of nanodiscs and polymers, respectively. M_D denotes the number of DPD beads in a nanodisc, for example, $M_D = 38$ for D5. In this work, φ_D varies from 0.01 to 0.15 and φ_P changes from 0 to 1. In the presence of polymers with $L_p = 12$, the nanodiscs may aggregate due to depletion force. In order to quantify the size of those aggregates, the weight-average aggregation number $\langle P_w \rangle$ is adopted

$$\langle P_w \rangle = \frac{\sum_i N_i P_i^2}{\sum_i N_i P_i} \tag{6}$$

Here P_i depicts the aggregation number of the ith cluster and N_i is the number of clusters with aggregation number P_i. The definition of a cluster is that any two DPD beads belong to the same cluster as the distance between them is less than a specific value, i.e., 0.7.

The depletion force between two nanodiscs is calculated. First, the interaction force between two nanodiscs, $\langle F \rangle$, is evaluated. As the separation between two nanodiscs (H) is given, the average forces acting on the two nanodiscs, which keep a set of constituent DPD beads fixed at $\{\mathbf{x}_1 \cdots \mathbf{x}_M\}$, are evaluated over all the configurations of all the remaining DPD beads (solvent and polymer) in the system with $\{\mathbf{x}_{M+1} \cdots \mathbf{x}_N\}$. The definition is given by[23]

$$\langle F \rangle(H) = \frac{\int F(\mathbf{x}_1 \cdots \mathbf{x}_M) e^{-\beta U(\mathbf{x}_1 \cdots \mathbf{x}_N)} \, d\mathbf{x}_{M+1} \cdots d\mathbf{x}_N}{\int e^{-\beta U(\mathbf{x}_1 \cdots \mathbf{x}_N)} \, d\mathbf{x}_{M+1} \cdots d\mathbf{x}_N} \tag{7}$$

Therefore, the mean force exerted on a nanodisc by the surrounding polymers and solvents is estimated by summing up all the forces acting on fixed DPD beads. For a symmetrical arrangement, the total force acting on the first nanodisc is essentially the same as that on the second one but in opposite direction. The separation-dependent interparticle force is then obtained by varying the interparticle distance. When the separation is far enough, the mean force acting on a nanodisc vanishes. Second, the repulsive force between two nanodiscs in the absence of solvent and polymer is calculated as $F_r(H)$. The depletion force (F_D) can then be determined by $F_D(H) = \langle F \rangle(H) - F_r(H)$. Note that the depletion force is caused by the deficiency of the depletant (solvent and polymer) in the depletion zone.

It is worth mentioning the limitations of the DPD simulation and, as a consequence, of the obtained results. The depletion interactions are based on the volume exclusion interactions for polymer (or solvent) in the local vicinity of the surface of the nanodiscs. While DPD has the advantage of being capable of dealing with large systems, it has a disadvantage of being a coarse-grained model. That is, multiple atoms or even molecules (e.g., water) are represented by a single bead, which is soft and partially penetrable. Both of these factors significantly hinder the accuracy of obtained results. Nonetheless, the qualitative behaviors of the phase diagram driven by depletion attraction can still be observed. In addition, DPD also offers valuable information which is independent of the microscopic molecular details. For example, the theoretical relation of $-F_D \propto (Dn)^2$, eqs 8 and 9, is examined by DPD simulations. The relevant results will be discussed in the next section.

III. RESULTS AND DISCUSSION

In the presence of nonadsorbing polymers, the nanodiscs may aggregate due to the depletion attraction. The depletion force between two nanodiscs is a function of disc diameter and polymer concentration. Their effects on depletion attraction are studied through calculating the force acting on the two nanodiscs at a given separation by DPD simulations. When the depletion attraction is strong enough, the aggregation of nanodiscs will take place. Depending on the size and concentration of nanodiscs and polymer concentration, three different phases are identified. The dynamic processes of different initial configurations are also observed to verify the final equilibrium outcomes.

dx.doi.org/10.1021/jp311657q | J. Phys. Chem. B XXXX, XXX, XXX−XXX

A. Depletion Force: Effect of Nanodisc Size. For dilute polymer solutions, the depletion attraction can be simply expressed as the product of polymer concentration (osmotic pressure) and the overlapped volume. At a specific polymer concentration, the depletion interaction is anticipated to be proportional to the overlapped volume, which is a function of the diameter of nanodiscs. Since the depletion force involves the interaction between polymers (solvents) and nanodiscs, it cannot be calculated directly and has to be obtained through ensemble average over all polymer (solvent) configurations. The effective force acting on the nanodiscs is first evaluated and demonstrated in the inset of Figure 2a. Like typical interparticle interaction, there exists a minimum and strong repulsion arises for closer separation. The effective force ($\langle F \rangle$) consists of the direct repulsion (F_r) between two nanodiscs and the depletion force (F_D) induced by polymers (solvents). Obviously, the presence of the attraction comes from the depletion attraction.

By subtracting the direct repulsion from the effective interaction, the depletion force is obtained, i.e., $F_D = \langle F \rangle - F_r$. Figure 2a shows the variation of the depletion force (F_D) with interparticle separation (H) for nanodiscs with different diameters (Dn) at $\varphi_P = 0.2$. When the two nanodiscs are far away, i.e., $H \gtrsim 1.1$, the polymer concentration between two nanodiscs is almost the same as that in the bulk solution. Hence, the depletion force is approximately equal to zero. As these two nanodiscs move closer, polymers and solvents are expelled out of the gap and thereby the concentration of polymer between two nanodiscs decreases. That is, for $H \lesssim 1.1$, the depletion strength ($-F_D$) grows monotonically. Moreover, the larger the nanodisc is, the greater the depletion strength is. Note that our model nanodisc is made of soft DPD beads and thus the depletion zone associated with the nanodisc is somewhat different from that of a hard disk.

The depletion interaction can be regarded as the result of the increment of the entropy associated with polymers and solvents. As the two nanodiscs gradually approach each other, the volume of overlapped zone is increased progressively while the available volume for the solvent and polymer (or the entropy of polymer and solvent) rises accordingly. The increment of the entropy reaches a maximum value once the excluded volume between them is completely overlapped. This point is corresponding to the minimum of the effective force at $H \simeq 0.85$, as shown in the inset of Figure 2a. In addition, the overlapped volume rises with the size of nanodiscs. As a consequence, at the same interparticle separation, the depletion force ($-F_D$) grows as the diameter of nanodiscs is increased.

Figure 2b shows the variation of the depletion force at $H = 0.9$ with the square of nanodisc diameter at different polymer concentrations. In dilute polymer solutions, the depletion interaction between two nanodiscs can be expressed as $F_D \approx (\varphi_P k_B T)\pi(Dn)^2$. Some features associated with the foregoing equation are observed in dilute and also concentrated solutions, as shown in Figure 2b. First of all, the depletion force is linearly proportional to the square of the nanodisc diameter ($(Dn)^2$) at a given polymer concentration. It indicates that the depletion zone is proportional to the disk area. Since the nanodisc is hexagonal in this work, the disk area is $(3(3)^{1/2}/8)(Dn)^2$. Second, the slope of the linear lines rises with increasing polymer concentration. This consequence reveals that the depletion force grows with the polymer concentration. The above results show the qualitative consistency between our simulations and the typical expression of the depletion force. However, Figure 2b also demonstrates that the increment of

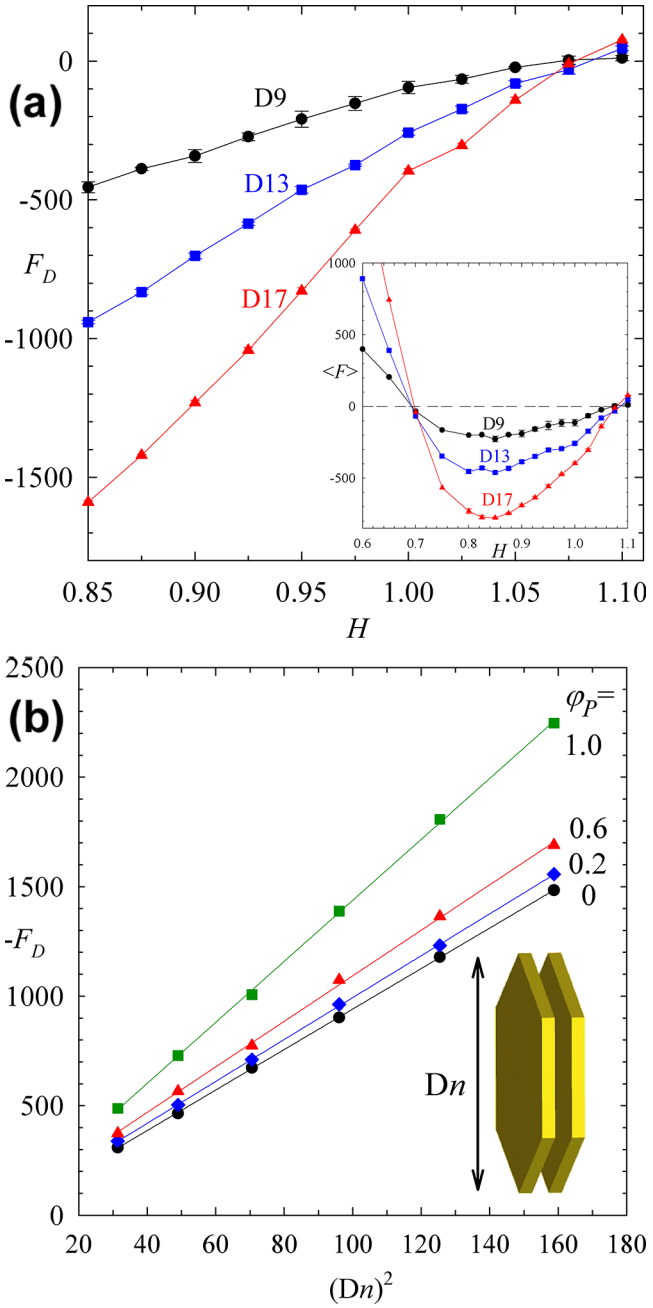

Figure 2. (a) The depletion force between two nanodiscs plotted against the interparticle separation at $\varphi_P = 0.2$. The effective interparticle force is given in the inset. (b) The variation of the depletion force ($-F_D$) at $H = 0.9$ with the square of nanodisc diameter at different polymer concentrations (φ_P).

the slope in the range of $\varphi_P \lesssim 0.6$ is less significant. Moreover, even in a pure solvent ($\varphi_P = 0$) or polymer melt ($\varphi_P = 1.0$), the depletion force follows the relation of $-F_D \propto (Dn)^2$. It implies that, in the absence of depletants, the depletion attraction can still be induced owing to the deficiency of solvent particles. Nonetheless, the depletion attraction is stronger in the polymer melt than that in the polymer solution.

B. Depletion Force: Effect of Polymer Concentration. At a fixed interparticle separation, the depletion force is enhanced as φ_P is increased. Figure 3 shows the variation of depletion force at $H = 0.9$ with polymer concentration for nanodisc D19. As $\varphi_P \lesssim 0.4$, the depletion force grows linearly

dx.doi.org/10.1021/jp311657q | J. Phys. Chem. B XXXX, XXX, XXX−XXX

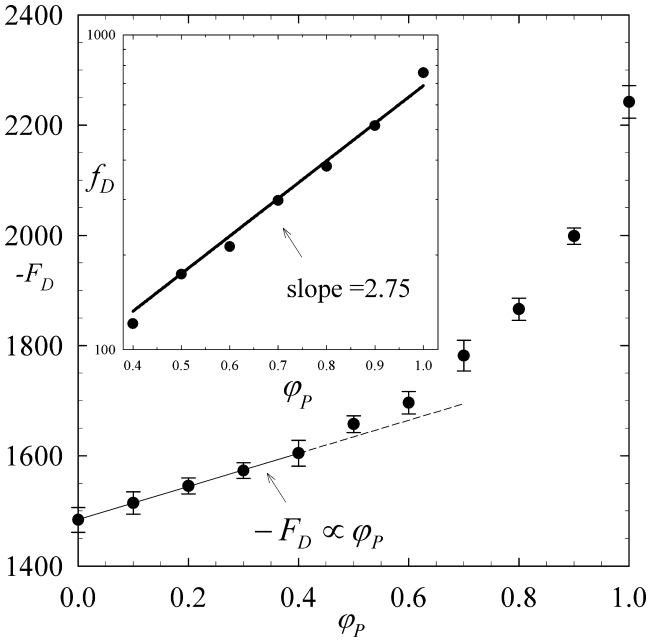

Figure 3. The variation of the depletion force at $H = 0.9$ with polymer concentration (φ_P) for nanodisc D19. In the inset, the enhanced depletion force due to polymer addition is plotted against polymer concentration.

with the polymer concentration and this result follows the expression of depletion attraction in the dilute polymer solution, in which the depletion potential is equal to the osmotic pressure times the overlapped volume. As the polymer concentration exceeds 0.4, the influence of φ_P on $-F_D$ is greater than linearity and rises rapidly as $\varphi_P \to 1$. Since the depletion attraction exists in a pure solvent as well, the total depletion force can be approximately expressed by $F_D(\varphi_P) = F_D(\varphi_P = 0) + f_D(\varphi_P)$ as nonadsorbing polymers are present in the solution. Here $f_D(\varphi_P)$ represents the enhanced depletion contribution associated with polymers and $f_D(0) = 0$. According to our simulation results, the depletion force induced by solvent only is $F_D(\varphi_P = 0) \simeq -1480$. In the range of $\varphi_P \lesssim 0.4$, $f_D(\varphi_P)$ is a linear function with the slope being 300 and thus one has $F_D \simeq -1510$ at $\varphi_P = 0.1$. Nonetheless, F_D becomes -2000 at $\varphi_P = 0.9$, which is significantly greater than $F_D(\varphi_P = 0) + f(\varphi_P = 0.9) = -1750$.

Since the depletion force is a linear sum of two terms, $F_D(\varphi_P = 0)$ and $f_D(\varphi_P)$, the overall depletion potential can be written as $A_D(\varphi_P) = A_D(\varphi_P = 0) + a_D(\varphi_P)$, where $A_D(\varphi_P = 0)$ and $a_D(\varphi_P)$ represent the depletion potential associated with pure solvent and polymer, respectively. In the dilute limit, it is known that

$$a_d(\varphi_p) = \Pi(\varphi_p)V_d \tag{8}$$

where Π is the osmotic pressure.[24] For a dilute polymer solution, the van't Hoff equation is usually valid and the osmotic pressure can be expressed as $\Pi = \varphi_P k_B T$. However, for a polymer solution in semidilute or concentrated regime, the validity of eq 8 is still unclear. It is reported that the osmotic pressure in the concentrated regime follows a power law, $\Pi/k_B T \sim \varphi_P^{\lambda}$, where λ depends on the chain length of the polymer.[25] The exponent approaches a constant, i.e., $\lambda = 2.73$, as the chain length is long enough. As shown in the inset of Figure 3, the data points are replotted in semilogarithmic form for $\varphi_P \geq 0.4$, $\ln(f_D)$ versus φ_P. The depletion force can be well represented by a straight line with a slope of about 2.75. The agreement of the exponent between the osmotic pressure and the depletion force reveals that the depletion force is also proportional to the osmotic pressure in the concentrated regime. That is, eq 8 may be true for any polymer concentration.

In general, the depletion interaction is not only affected by the nanodisc size and polymer concentration but also by the size of depletants. In order to understand how the depletant size influences the depletion interaction, the depletion force is plotted against the interparticle separation for pure solvent ($L_p = 1$ and $\varphi_P = 0$) and polymer melt ($L_p = 12$ and $\varphi_P = 1.0$), as shown in Figure 4. For polymer melt, the depletion force

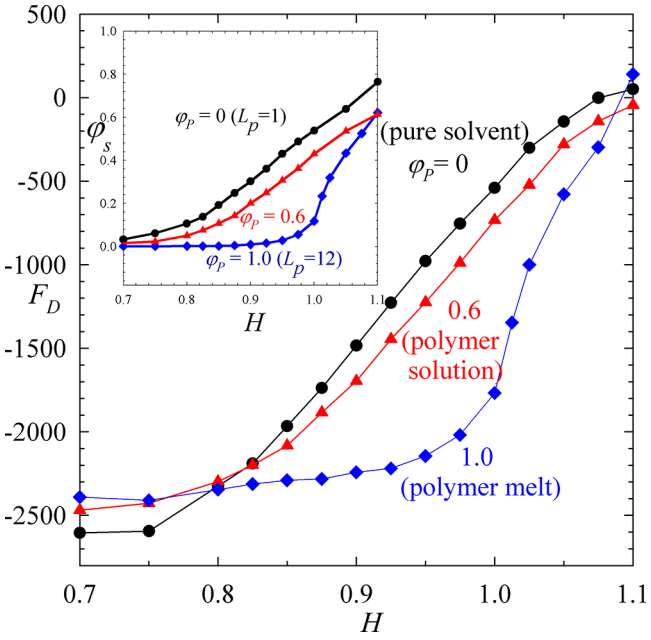

Figure 4. The variation of the depletion force between nanodiscs D19 with interparticle separation. In the inset, the volume fraction of polymers and solvents within the gap (φ_s) is plotted against interparticle separation.

($-F_D$) grows significantly with decreasing interparticle separation at $0.95 \lesssim H \lesssim 1.1$. As the two nanodiscs approach even closer, i.e., $H \lesssim 0.95$, the increment of depletion force is insignificant. That is, the depletion force is approximately a constant at this range. However, for small solvent, the depletion strength grows continuously and reaches a plateau at about $H \simeq 0.75$. This result indicates that the size of the solvent beads has a significant influence on the interaction range.

At a specific interparticle separation, the depletion interaction between two nanodiscs depends on the difference of the depletant concentration inside and outside the overlapped depletion zone. For smaller solvent ($L_p = 1$), the solvent particles can be found inside the overlapped zone even at a small separation such as $H = 0.75$, as shown in the inset of Figure 4, where φ_s denotes the volume fraction of polymers and solvents within the gap. However, for a larger solvent such as polymer ($L_p = 12$), they are too bulky to exist in the overlapped region, as the interparticle separation is less than 0.95. In other words, the maximum depletion force between two nanodiscs in polymer melt is reached at larger separation compared to that in small solvent, i.e., at $H = 0.75$. Note that, for a mixture of small solvent and polymer (i.e., polymer solution), the

dx.doi.org/10.1021/jp311657q | J. Phys. Chem. B XXXX, XXX, XXX−XXX

contribution of small solvent generally dominates over that of polymer because of the larger number density associated with small solvent. As demonstrated in Figure 4, the depletion force for $\varphi_P = 0.6$ is very close to that for $\varphi_P = 0$. Moreover, it is also found that F_D is closely related to the volume fraction of polymer/solvent in the gap. By plotting F_D against φ_s, a linear relation between them is obtained. This consequence reveals that it is generally a common feature of depletion attraction due to osmotic pressure difference.

C. Phase Separation and Structure. Depletion forces provide attraction between solvophilic nanoparticles which are dispersed uniformly in the absence of nonadsorbing polymers. Similar to phase separation associated with the mixture of simple fluids due to van der Waals attraction, it is anticipated that phase separation may occur for the dispersion of solvophilic nanoparticles driven by polymer addition. That is, by varying polymer concentration (corresponding to interaction strength) and nanoparticle concentration (corresponding to composition), there may exist at least two equilibrium states, dispersion and phase separation. Evidently, dispersion is anticipated for low φ_P and φ_D and phase separation is expected for high φ_P and φ_D.

Figure 5 shows the snapshot of equilibrium states of nanodiscs in semidilute ($\varphi_P = 0.01$) and concentrated ($\varphi_P =$ 0.5) polymer solutions. For small φ_P as depicted in Figure 5a, the depletion force is too weak to drive the cluster formation. As a result, nanodiscs distribute homogeneously in the solution to increase the particle entropy. On the contrary, for large φ_P as illustrated in Figure 5b, almost all the nanodiscs in the system aggregate together because of strong depletion attraction. Phase separation is mainly driven by polymer entropy. The two phases can be regarded as a nanodisc-rich phase and a solvent (polymer)-rich phase. Note that the nanoparticle concentration is in the dilute regime ($\varphi_D = 0.03$) for the former case, while it is in the semidilute regime for the latter case ($\varphi_D = 0.08$).

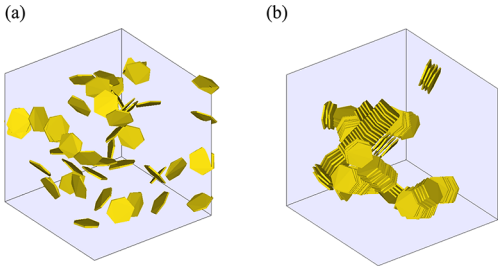

Figure 5. Snapshots of the aggregation outcomes of solvophilic nanodisc D19 in polymer solution: (a) $\varphi_P = 0.01$ and $\varphi_D = 0.03$; (b) $\varphi_P = 0.5$ and $\varphi_D = 0.08$.

In order to examine the thermodynamic stability of the dispersed state and phase separation, DPD simulations starting with two initial configurations of nanodiscs are preformed at the same φ_P and φ_D. As demonstrated in Figure 6, the dispersed state is always obtained, irrespective of the initial configuration being a random distribution or an ordered aggregate arrangement. Note that the initial value of the aggregation number is 1 for the randomly distributed structure and 46 for the ordered aggregate, respectively. For the former case, the aggregation number remains unity during the simulation. For the latter case, however, the aggregation number decays rapidly and it reaches unity as $2 \times 10^4\ \Delta t$. This result shows that a dilute dispersion of nanodiscs in a dilute polymer solution is thermodynamically favorable. Different from the behavior of nanodiscs in the dilute polymer solution, the mean aggregation number of nanodiscs grows gradually with time in a concentrated polymer solution for an initially random configuration. The aggregation process is shown in the inset of Figure 6. On the other hand, for an initially ordered aggregate configuration with $\langle P_w \rangle = 122$, the state of phase separation remains unchanged but the structure is adjusted during the simulation. Another approach to examine the stability of phase separation is to introduce a perturbation into the system with a pre-existing nanodisc-rich phase by redissolving a few nanodiscs. Eventually, free nanodiscs readsorb onto the large aggregate and vanish. Hence, for higher values of φ_P and φ_D, the system prefers to be phase-separated thermodynamically. It is worth mentioning that it requires a long time to reach the phase-separated state, i.e., $t \sim 10^6\ \Delta t$, if nanodiscs are initially dispersed.

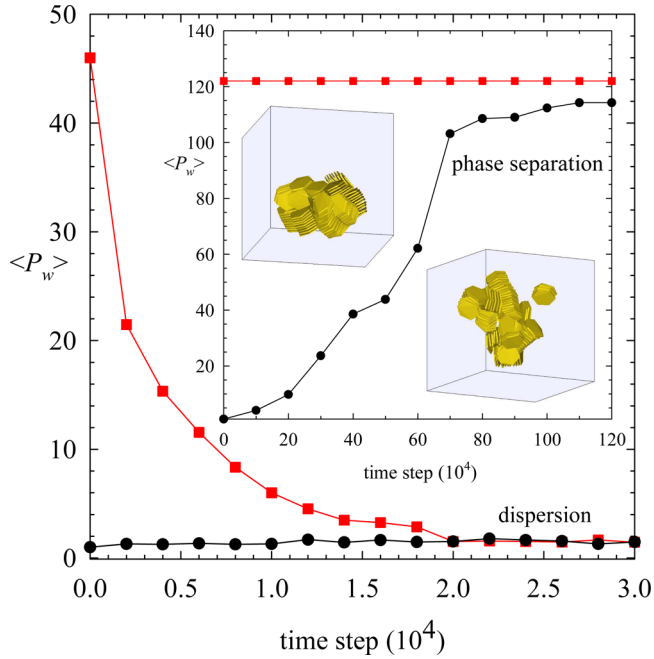

Figure 6. The variation of mean aggregation number with time step for two different initial configurations. Dispersion is observed for $\varphi_P = 0.01$ and $\varphi_D = 0.03$. In the inset, phase separation is seen for $\varphi_P = 0.5$ and $\varphi_D = 0.08$.

When phase separation occurs, the arrangement of the nanodisc-rich phase must differ distinctly from that of spherical nanoparticles. On the basis of the radial distribution function, the self-assembly structure of nanodiscs due to depletion attractions is shown. As illustrated in Figure 5b, the nanodisc-rich phase consists of several column-like structures which are formed by the regular stack of nanodiscs in a face-to-face manner. In this case, the radial distribution function $g(r)$ should exhibit periodic peaks and this inference is confirmed in Figure 7. The peak located at $r = 1.5$ corresponds to the two contact nanodiscs, and the peak at $r = 3.0$ is with respect to the two nanodiscs separated by one nanodisc. Similarly, the peaks at $r = 4.5$ or $1.5m$ denote the two nanodiscs separated by two or $(m - 1)$ nanodiscs. In addition to the face-to-face configuration, each column-like structure may also stack in a face-to-side configuration due to the strong depletion. As a consequence, the small peak appearing at $r \approx 6.2-6.8$ represents the face-to-side configuration. This result reveals that, during the process of

dx.doi.org/10.1021/jp311657q | J. Phys. Chem. B XXXX, XXX, XXX−XXX

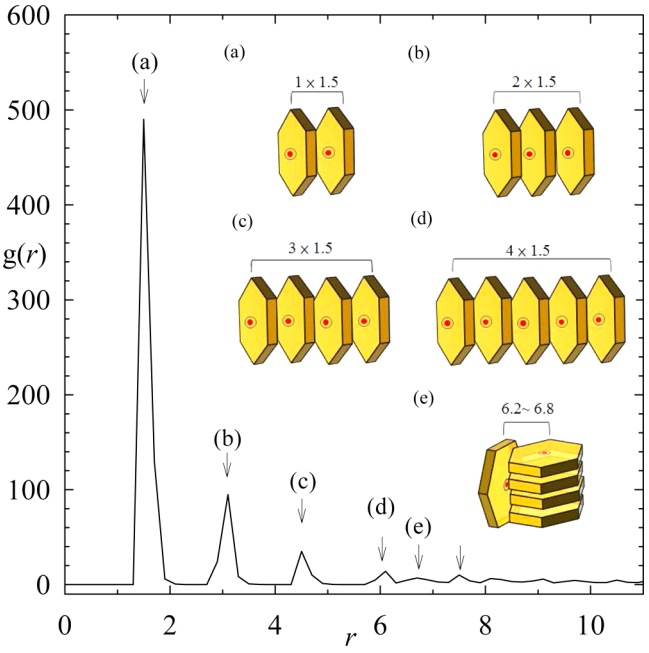

Figure 7. The structure of the self-assembly of nanodisc D19 analyzed by the radial distribution function at $\varphi_P = 0.5$ and $\varphi_D = 0.08$.

phase separation, column-like structures form first and the face-to-side structures appear later on. The average number of nanodiscs associated with column-like structures in the nanodisc-rich phase is about 6, and it can be realized from the nearly vanishing peak associated with face-to-face arrangement at $r \approx 7.5$.

D. Pretransition Regime: Finite Sized Clusters. According to the simulation results in the foregoing section, the nanodiscs disperse at small φ_P and φ_D, while the phase separation takes place at large φ_P and φ_D. The naturally arising question is as follows: Is there a pretransition regime between dispersion and phase separation? That is, will finite sized clusters of nanodiscs be stably suspended in this regime? In addition, since the strength of depletion attraction is a function of nanodisc size and concentration as well as polymer concentration, can the mean size of aggregates of nanodiscs be controlled by tuning those parameters? Our simulation results show that, different from the morphologies of dispersion and phase separation, column-like clusters are clearly observed in the polymer concentration regime, $0.15 \lesssim \varphi_p \lesssim 0.5$, as illustrated in Figure 8 for solvophilic nanodiscs D13 ($\varphi_D = 0.07$) at two polymer concentrations. By the comparison between Figure 8a and b, the mean size of aggregates seems to

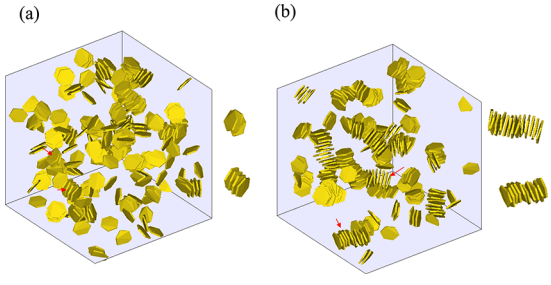

Figure 8. Snapshots of the degree of aggregation associated with solvophilic nanodiscs D13 at $\varphi_D = 0.07$ for (a) $\varphi_P = 0.15$ and (b) $\varphi_P = 0.2$.

grow with increasing polymer concentration. In order to explore the thermodynamic stability associated with the nanodisc clusters in the pretransition regime, the time variation of mean aggregation number is plotted for two initial configurations. As shown in the Supporting Information (Figure S1), the mean aggregation number decays from an ordered structure with $\langle P_w \rangle = 162$. On the other hand, the mean aggregation number grows from a random structure with $\langle P_w \rangle = 1$. However, no matter what the initial configurations are, the mean aggregation number approaches a constant, i.e., $\langle P_w \rangle \approx 8.5$, after the system reaches thermodynamic equilibrium, i.e., $t > 8 \times 10^5$. This result implies that, independent of the initial configurations, the finite sized aggregates are always observed. Therefore, the pretransition regime is thermodynamically stable. Note that this mean aggregation number corresponds to $\varphi_P = 0.15$ and $\varphi_D = 0.05$.

The occurrence of aggregation or dispersion associated with colloidal particles is typically determined by the competition between internal energy and entropy ($T\Delta S$) of the system. Basically, colloidal particles tend to disperse in the solution to increase the translational entropy (ΔS_{trans}). Thereby, dispersion is driven by translational entropy. On the contrary, the existence of a significant attractive force will drive the formation of aggregates of colloidal particles due to reduction of internal energy. As a result, aggregation is dominant by internal energy. In our system, although interparticle attractions between solvophilic nanodiscs are absent, an attractive force is still induced by the depletion of polymers (and solvents). The attractive force is also of entropic origin. Hence, the aggregation of solvophilic nanodiscs is simply driven by the increase of solution entropy associated with the depletion effect (ΔS_{dep}). At a fixed polymer concentration, the equilibrium state of the nanodisc solution varies with the nanodisc concentration and it depends on whether ΔS_{trans} or ΔS_{dep} dominates. For dilute nanodisc solutions, ΔS_{trans} dominates over ΔS_{dep} and thus nanodiscs suspend uniformly in the solution. As the nanodisc concentration is increased, the importance of ΔS_{trans} declines, while aggregation can result in an increase of ΔS_{dep}. Therefore, when φ_D is high enough, the increase in ΔS_{dep} wins over the ΔS_{trans} loss and clusters of nanodiscs begin to form. Note that the formation of finite sized clusters indicates the self-assembly of nanodiscs, instead of phase separation. Such a self-assembled behavior of nanodiscs is somewhat similar to that of the formation of finite sized micelles of surfactant.

Typically, the onset of surfactant micellization in terms of critical micelle concentration (CMC) is determined by plotting the free surfactant concentration as a function of the total surfactant concentration. The CMC is then defined as the free surfactant concentration which remains constant. Figure 9 shows the variation of free nanodisc concentration (φ_D^f) with overall nanodisc concentration (φ_D) for various nanodisc sizes (Dn). Since nanodiscs prefer to form a column-like structure in the pretransition regime as seen in Figure 8, the free nanodisc concentration (φ_D^f) shown in Figure 9 is obtained by the subtracting nanodisc concentration associated with face-to-face clusters from φ_D. Note that here the two nanodiscs are considered in a face-to-face cluster only when the distance between their center of mass is less than 2. When the size of the nanodisc is small, such as D5 and D9, φ_D^f is essentially equal to φ_D as $\varphi_D \lesssim 0.15$ and this result indicates that the system is in a dispersed state. That is, the depletion force is weak for small nanodiscs and ΔS_{trans} dominates over ΔS_{dep}. The fact that φ_D^f deviates slightly from φ_D for nanodisc D9 reveals that dimers or

dx.doi.org/10.1021/jp311657q | J. Phys. Chem. B XXXX, XXX, XXX−XXX

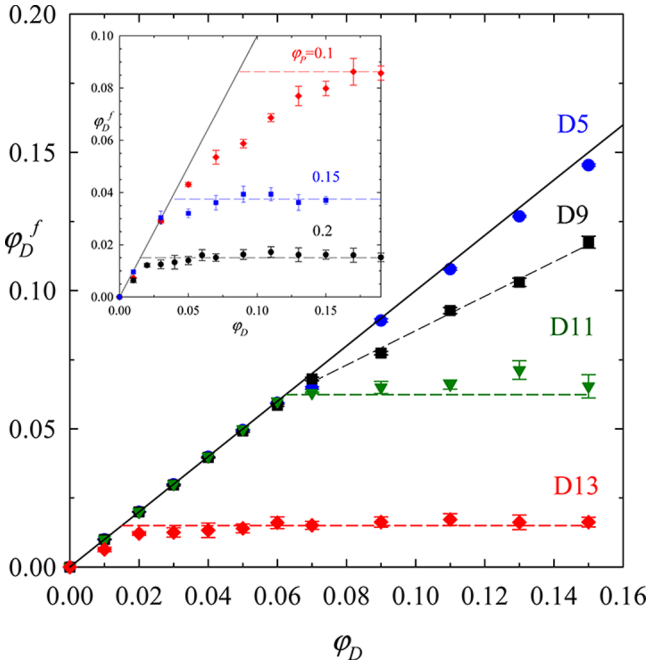

Figure 9. The volume fraction of free nanodiscs (φ_D^f) versus the total volume fraction of nanodiscs (φ_D) at φ_P = 0.2 for different sizes of nanodiscs. In the inset, φ_D^f is plotted against φ_D for nanodisc D13 at different φ_P.

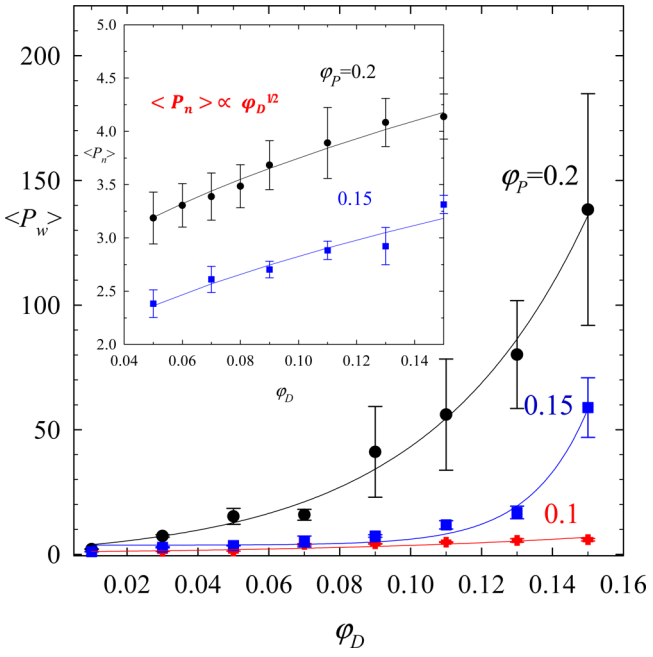

Figure 10. The variation of mean aggregation number with nanodisc concentration for nanodisc D13 at different polymer concentrations. In the inset, the mean size of columnar clusters is plotted against nanodisc concentration.

trimers of nanodiscs start to form. On the contrary, as φ_D is increased for large nanodiscs including D11 and D13, the free nanodisc concentration grows linearly for low nanodisc concentration and then becomes independent of φ_D for high enough concentration. Evidently, the formation of nanodisc clusters indicates that ΔS_{dep} wins over ΔS_{trans} at high enough φ_D.

Following the concept of CMC, the constant value of free nanodisc concentration in the pretransition regime is defined as the critical aggregation concentration (CAC). Since the value of the CMC typically declines with increasing intermolecular attraction between surfactants,[26] the CAC value is anticipated to decrease as the nanodisc size grows. Therefore, as illustrated in Figure 9, the CAC of nanodisc D13 is lower than that of nanodisc D11 because the depletion attraction of the former is stronger. This consequence implies that, for a given polymer concentration, the larger the nanodisc, the smaller the onset concentration of the pretransition regime. Similarly, for the same size of nanodisc, since the strength of interparticle interaction (or depletion force) grows with increasing polymer concentration, the CAC is expected to decay with increasing φ_P. As demonstrated in the inset of Figure 9, the CAC follows the order $c_{0.2} < c_{0.15} < c_{0.1}$, where c_{φ_P} denotes the CAC of nanodisc D13 at φ_P.

E. Cluster Size and Phase Diagram. Since the self-assembly of nanodiscs is a collective behavior, the size of clusters may be influenced by the nanodisc concentration in the pretransition state. Figure 10 shows the variation of the mean aggregation number ($\langle P_w \rangle$) with nanodisc concentration of D13 at different polymer concentrations. Note that the mean aggregation number is evaluated on the basis of the statement that any two nanodiscs in contact belong to the same cluster, as described in section II. Therefore, an aggregate may consist of T-shaped structures of columns or side-by-side bundles of nanodiscs. Obviously, the mean aggregation number grows with increasing nanodisc concentration at a specific polymer concentration. When the polymer concentration is low, i.e., φ_P = 0.1, the depletion attraction is relatively weak, and therefore, $\langle P_w \rangle$ grows slightly with increasing φ_D. As the polymer concentration is high enough, further increasing nanodisc concentration results in significant increment of mean aggregation number. Moreover, since the depletion attraction grows with φ_P, $\langle P_w \rangle$ is anticipated to rise as φ_P is increased at a given φ_D. For instance, for φ_D = 0.11, $\langle P_w \rangle \approx 12$ at φ_P = 0.15 but $\langle P_w \rangle \approx 56$ at φ_P = 0.2. These results reveal that the cluster size can be tuned by the amount of added polymers.

From a thermodynamical point of view, the necessary condition for the formation of stable aggregates is that the mean chemical potential of a particle in the aggregated state is always less than that in the dispersed state. On the basis of particle−particle bond energy in the aggregate and the structure formed by the association of identical particles,[27] the chemical potential can be estimated. It is found that the nature of aggregates depends significantly on their dimensionality and geometry. For two- and three-dimensional aggregates, there is a phase transition from a dispersion to a separate phase (or an aggregate of infinite size) as the particle concentration exceeds a specific value, e.g., CMC for surfactant. However, in the case of one-dimensional structures of aggregates such as rods and cylinders, a distribution of finite sized clusters is always seen. It is typically referred to as micellization, in contrast to infinite aggregates (phase separation). When the particle concentration is greater than the CMC, the number-average aggregation number ($\langle P_n \rangle$) can be derived from the chemical potential argument[27]

$$\langle P_n \rangle \approx 2\sqrt{\varphi e^{\alpha}} \tag{9}$$

where φ represents the volume fraction of particles and α denotes a positive constant associated with the strength of the interparticle interactions. Although eq 9 is generally applied to

dx.doi.org/10.1021/jp311657q | J. Phys. Chem. B XXXX, XXX, XXX−XXX

surfactant systems,[27] it can be regarded as the thermodynamic principle of one-dimensional self-assembly by any attractive force.

Evidently, the dimensionality of column-like clusters observed in the pretransition regime is equal to unity and thus the self-assembled behavior of nanodisc may be described by eq 9. That is, the mean size of column-like aggregates formed by nanodiscs is expected to vary with the square root of nanodisc concentration and to grow with increasing depletion attraction. The inset of Figure 10 shows the variation of number-average aggregation number ($\langle P_n^c \rangle$) of columnar clusters with nanodisc concentration (φ_D) above the CAC at a given polymer concentration (or a specific α). The simulation data points can be reasonably represented by the theoretical solid line, $\langle P_n^c \rangle \propto \varphi_D^{1/2}$. In addition, $\langle P_n^c \rangle$ rises with increasing φ_P, which corresponds to the increment of α. The foregoing result implies that eq 9 derived from one-dimensional aggregates can in principle work for describing depletion-induced self-assembly of nanodiscs to form columnar clusters.

It is worth noting that there is a significant difference between $\langle P_w \rangle$ and $\langle P_n^c \rangle$ in Figure 10. For example, $\langle P_w \rangle \approx 140$ but $\langle P_n^c \rangle \approx 4$ at $\varphi_D = 0.15$ and $\varphi_P = 0.2$. Since $\langle P_n^c \rangle$ is rigorously defined for the columnar structure only, two neighboring nanodiscs belonging to the same cluster must satisfy the condition that the distance between their center of mass is less than 2. On the contrary, $\langle P_w \rangle$ is adopted for an aggregate with any shape and thereby any two nanodiscs in contact belong to the same aggregate. In the pretransition regime, the clusters dispersed in the system are mainly in a column-like fashion, as shown in Figure 8. T-shaped structures of columns may also be observed. Evidently, $\langle P_w \rangle \approx \langle P_n^c \rangle$ if T-shaped structures are absent. At higher nanodisc concentration, the contacts among T-shaped structures of columns result in large aggregates. As a result, $\langle P_w \rangle \gg \langle P_n^c \rangle$. This consequence reveals that T-shaped structures of columns are more favorable than a single column because the face-to-side depletion attraction becomes important at higher φ_D.

Obviously, the equilibrium state depends on φ_P and φ_D, and the morphological phase diagram can be realized by $\langle P_n^c \rangle$ and $\langle P_w \rangle$. In the dispersed phase, the translational entropy of nanodiscs prevails and $\langle P_n^c \rangle \approx 0$. In the pretransition phase, the face-to-face depletion attraction becomes dominant and $\langle P_n^c \rangle \gtrsim 2$. When almost all of the nanodiscs aggregate together to form a bundle of columns or a pack of columns, as depicted in Figure 5, the system is claimed to be phase-separated. In such a case, $\langle P_w \rangle$ is close to the total number of nanodiscs in our simulation system, while $\langle P_n^c \rangle$ representing the mean column length is still small. The depletion attractions associated with face-to-side and side-to-side arrangements also come into play. The interparticle attraction with entropic origin predominates over translational entropy.

Our simulation results indicate that the equilibrium state changes from dispersion to pretransition, and then to phase separation, as the polymer concentration and nanodisc concentration are increased. Such phase transitions are driven by the increment of depletion attraction (ΔS_{dep}) and the decrement of nanodisc translational entropy (ΔS_{trans}). Similar to the formation of micelles by surfactants, the critical aggregation concentration (CAC) can be used to distinguish dispersion from pretransition. That is, at a given nanodisc size and polymer concentration, dispersion occurs for $\varphi_D <$ CAC and pretransition takes place for $\varphi_D >$ CAC. This criterion for the transition from dispersion to pretransition can be examined from the variation of the mean aggregation number with nanodisc concentration. As shown in Figure S2 (Supporting Information), for a suspension of nanodisc D19 at $\varphi_P = 0.05$, the CAC corresponding to a constant value of φ_D^f is about 0.03. In the inset of Figure S2 (Supporting Information), the transition concentration can also be characterized by the intersection point of the two lines depicting $\langle P_w \rangle = f(\varphi_D)$ in the two different states. Evidently, the transition concentration determined from the plot of free nanodiscs is consistent with that from the plot of the mean aggregation number.

The phase transition from pretransition state to phase-separated state can be characterized by the normalized aggregation number ($\langle P_w \rangle / N_D$) and reduced averaged cluster size. The reduced averaged cluster size is defined as[28]

$$I_{av} = \frac{\sum_i N_i P_i^2 - {P_{max}}^2}{\sum_i N_i P_i} \tag{10}$$

where P_{max} represents the aggregation number of the largest cluster. In the pretransition state, since P_{max} is relatively small, the reduced averaged cluster size behaves similarly to $\langle P_w \rangle$. Therefore, at a given polymer concentration, I_{av} grows with increasing φ_D. In the phase-separated state, however, the mean aggregation number is dominated by the largest cluster, resulting in a small value of I_{av} close to zero. Consequently, the transition concentration can be determined by the concentration associated with the sharp decrement of I_{av}. For a suspension of nanodisc D19 at $\varphi_P = 0.2$, the onset of phase-separated state is $\varphi_D \approx 0.07$, as pointed to by the arrow in the inset of Figure S3 (Supporting Information). This result agrees with the transition concentration ($\langle P_w \rangle / N_D \rightarrow 1$) obtained from Figure S3 (Supporting Information) for the normalized mean aggregation number.

The equilibrium state of a nanodisc suspension depends on φ_P and φ_D. On the basis of the criteria associated with phase transition, the morphological phase diagram for nanodisc D19 is constructed by varying φ_P between 0.01 and 0.4 and φ_D between 0.01 and 0.1, as shown in Figure 11. The phase

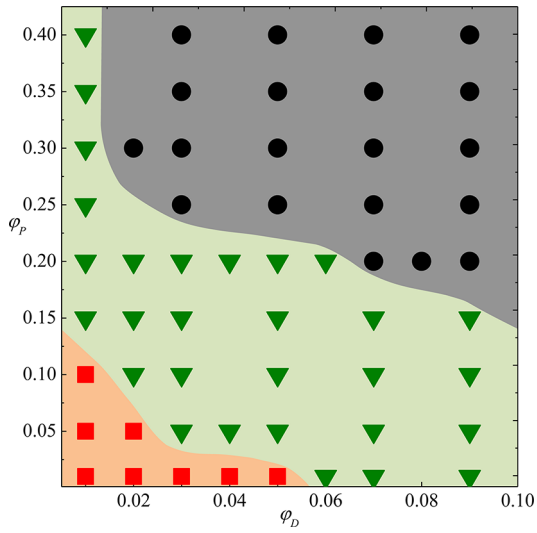

Figure 11. Morphological phase diagram for nanodisc D19. The equilibrium state is a function of polymer concentration (φ_D) and nanodisc concentration (φ_P). The filled square, triangle, and circle symbols represent dispersion, pretransition, and phase separation regions, respectively.

dx.doi.org/10.1021/jp311657q | J. Phys. Chem. B XXXX, XXX, XXX−XXX

diagram is essentially characterized by the boundary curves between different regions, $\varphi_P^* = g_{d\to p}(\varphi_D)$ and $\varphi_P^* = g_{p\to s}(\varphi_D)$. The dispersion region (d) is observed at low φ_P and φ_D, while the phase separation region (s) is seen at high φ_P and φ_D. The pretransition region (p) is located in the intermediate region between dispersion and phase separation. In general, φ_P^* decreases with increasing φ_D for both transitions, d → p and p → s. That is, the phase transition requires less amount of nonadsorbing polymers at higher nanodisc concentrations. It should be noted that the phase diagram also varies with nanodisc size. Since the depletion force grows with increasing nanodisc size, the phase boundary curves are anticipated to shift upward for smaller nanodiscs. That is, the dispersion region will expand but the phase separation region will shrink in the phase diagram of small nanodiscs.

IV. CONCLUSION

The entropic attraction between *anisotropic* nanoparticles can be induced by polymer addition. Though it is stronger than that between nanospheres, the relevant work is still limited. In this study, in the presence of nonadsorbing polymers, the depletion interaction between two solvophilic nanodiscs and the aggregation behavior of a suspension of nanodiscs are investigated by DPD simulations. The depletion attraction is influenced by polymer concentration, nanodisc size, and nanodisc concentration. The equilibrium state of a nanodisc suspension can be classified into dispersion, pretransition associated with finite sized clusters, and phase separation. The morphological phase diagram is then constructed by observing the size and structure of aggregates formed by nanodiscs at different φ_P and φ_D.

The effective attraction between two solvophilic nanodiscs can be simply obtained from simulation, and the depletion attraction is calculated by subtraction of the direct interparticle repulsion. The depletion force is proportional to the area of the nanodisc and grows with increasing polymer concentration. Note that the depletion interaction still exists even in the absence of depletants (polymers). Thus, the addition of polymers enhances the depletion potential by osmotic pressure, $A_D(\varphi_P) = A_D(\varphi_P = 0) + a_D(\varphi_P)$. The depletion potential associated with depletants (a_D) can be written as the product of osmotic pressure ($\varphi_P^\lambda k_B T$) and the excluded volume of the nanodiscs (V_D), i.e., $a_D(\varphi_P) \sim (\varphi_P^\lambda k_B T)V_D$. The exponent is λ = 1 in dilute polymer solution, while it grows to be λ = 2.75 in concentrated solution. In other words, the depletion attraction increases linearly in a dilute regime but grows significantly with φ_P in a concentrated regime. Note that it can be useful to understand the effects of polymer properties (e.g., length, conformation, and rigidity) on the depletion interactions. Those effects are currently under study.

By increasing polymer and nanodisc concentrations, the equilibrium state of a nanodisc suspension changes from dispersion to pretransition, and then to phase separation. Although the molecular structure of a surfactant characterized by a solvophilic head and a solvophobic tail is distinctly different from that of a nanodisc, the self-assembled behavior of a nanodisc in the pretransition regime resembles that of a surfactant. That is, when the nanodisc concentration exceeds the CAC, finite sized clusters of nanodiscs are formed. The value of CAC decays with increasing depletion attraction. The primary structure of aggregates is column-like owing to the face-to-face depletion attraction. Moreover, the variation of number-average aggregation number with nanodisc concentration can be in principle depicted by the simple thermodynamic model for a one-dimensional aggregate. On the other hand, for phase separation, a nanodisc-rich phase formed by a bundle of columns or a pack of columns is seen owing to strong depletion attractions among columnar clusters in face-to-side and side-to-side manners.

■ ASSOCIATED CONTENT

Supporting Information

The variation of mean aggregation number with time step for two different initial configurations in the pretransition regime (φ_P = 0.15 and φ_D = 0.05) where finite sized clusters are formed. The variation of volume fraction of free nanodisc (φ_D^f) with total volume fraction of nanodisc (φ_D) for nanodisc D19 at φ_P = 0.05. The plot of mean aggregation number against total volume fraction of nanodisc. The variation of normalized mean aggregation number ($\langle P_w\rangle/N_D$) with total volume fraction of nanodisc (φ_D) for nanodisc D19 at φ_P = 0.2. The plot of reduced averaged cluster size (I_{av}) against total volume fraction of nanodisc. This material is available free of charge via the Internet at http://pubs.acs.org.

■ AUTHOR INFORMATION

Corresponding Author

*E-mail: yjsheng@ntu.edu.tw (Y.-J.S.); hktsao@cc.ncu.edu.tw (H.-K.T.).

Notes

The authors declare no competing financial interest.

■ ACKNOWLEDGMENTS

This research work is supported by National Science Council of Taiwan. Computing times, provided by the National Taiwan University Computer and Information Networking Center and National Center for High-Performance Computing (NCHC) are gratefully acknowledged.

■ REFERENCES

(1) Mason, T. G. Osmotically Driven Shape-Dependent Colloidal Separations. *Phys. Rev. E* **2002**, *66*, 060402.
(2) Rossi, L.; Sacanna, S.; Irvine, W. T. M.; Chailin, P. M.; Pine, D. J.; Philipse, A. P. Cubic Crystals from Cubic Colloids. *Soft Matter* **2011**, *7*, 4139−4142.
(3) Schwarz-Linek, J.; Valeriani, C.; Ctes, M. E.; Morenduzzo, D.; Morozov, A. N.; Poon, W. C. K. Phase Separation and Rotor Self-Assembly in Active Particle Suspensions. *Proc. Natl. Acad. Sci. U.S.A.* **2012**, *109*, 4052−4057.
(4) Asakura, S.; Oosawa, F. Interaction between Particles Suspended in Solutions of Macromolecules. *J. Polym. Sci.* **1958**, *33*, 183−192.
(5) Dogic, Z.; Fraden, S. Ordered Phases of Filamentous Viruses. *Curr. Opin. Colloid Interface Sci.* **2006**, *11*, 47−55.
(6) Kyoungweon, P.; Hilmar, K.; Richard, A. V. Depletion-Induced Shape and Size Selection of Gold Nanoparticles. *Nano Lett.* **2010**, *10*, 1433−1439.
(7) Goodwin, J. W. *Colloids and Interfaces with Surfactants and Polymers*; John Wiley & Sons: Hoboken, NJ, 2004.
(8) Israelachvili, J. N. *Intermolecular & Surface Forces*; Academic Press: London, 1991.
(9) Tuinier, R.; Vliegenthart, G. A.; Lekkerkerker, H. N. W. Depletion Interaction between Spheres Immersed in a Solution of Ideal Polymer Chains. *J. Chem. Phys.* **2000**, *113*, 10768−10775.
(10) Hoogerbrugge, P. J.; Koelman, J. M. V. A. Simulating Microscopic Hydrodynamic Phenomena with Dissipative Particle Dynamics. *Europhys. Lett.* **1992**, *19*, 155−160.

(11) Groot, R. D.; Warren, P. B. Dissipative Particle Dynamics: Bridging the Gap between Atomistic and Mesoscopic Simulation. *J. Chem. Phys.* **1997**, *107*, 4423−4435.
(12) Espanol, P.; Warran, P. B. Statistical Mechanics of Dissipative Particle Dynamics. *Europhys. Lett.* **1995**, *30*, 191−196.
(13) Huang, K. C.; Lin, C. M.; Tsao, H. K.; Sheng, Y. J. The Interactions between Surfactants and Vesicles: Dissipative Particle Dynamics. *J. Chem. Phys.* **2009**, *130*, 245101.
(14) Singh, A.; Jayabalan, J.; Chari, R.; Srivastava, H.; Oak, S. M. Tuning the Localized Surface Plasmon Resonance of Silver Nanoplatelet Colloids. *J. Phys. D: Appl. Phys.* **2010**, *43*, 335401.
(15) Shen, J.; Hu, Y.; Li, C.; Qin, C.; Shi, M.; Ye, M. Layer-by-Layer Self-Assembly of Graphene Nanoplatelets. *Langmuir* **2009**, *25*, 6122−6128.
(16) Xu, S.; Whitin, J. C.; Yu, T. T. S.; Zhou, H.; Sun, D.; Sue, H. J.; Zou, H.; Cohen, H. J.; Zare, R. N. Capture of Phosphopeptides Using α-Zirconium Phosphate Nanoplatelets. *Anal. Chem.* **2008**, *80*, 5542−5549.
(17) Gaharwar, A. K.; Schexnailder, P.; Kaul, V.; Akkus, O.; Zakharov, D.; Seifert, S.; Schmid, G. Highly Extensible Bio-Nanocomposite Films with Direction-Dependent Properties. *Adv. Funct. Mater.* **2010**, *20*, 429−436.
(18) Hu, S. W.; Sheng, Y. J.; Tsao, H. K. Self-Assembly of Organophilic Nanoparticles in a Polymer Matrix: Depletion Interactions. *J. Phys. Chem. C* **2012**, *116*, 1789−1797.
(19) Li, Y. L.; Chiou, C. S.; Kumar, S. K.; Lin, J. J.; Sheng, Y. J.; Tsao, H. K. Self-Assembled Superstructures of Polymer-Grafted Nanoparticles: Effects of Particle Shape and Matrix Polymer. *J. Phys. Chem. C* **2011**, *115*, 5566−5577.
(20) Nakajima, T.; Hirao, K. A Dual-Level Approach to Density-Functional Theory. *J. Chem. Phys.* **2006**, *124*, 184108.
(21) Chou, S. H.; Tsao, H. K.; Sheng, Y. J. Structural Aggregations of Rod-Coil Copolymer Solutions. *J. Chem. Phys.* **2011**, *134*, 034904.
(22) Sheng, Y. J.; Wang, T. Y.; Chen, W. M.; Tsao, H. K. A-B Diblock Copolymer Micelles: Effects of Soluble-Block Length and Component Compatibility. *J. Phys. Chem. B* **2007**, *111*, 10938.
(23) Chandler, D. *Introduction to Modern Statistical Mechanics*; Oxford University Press: New York, 1987.
(24) Philips, R.; Kondev, J.; Theriot, J.; Orme, N. *Physical Biology of the Cell*; Garland Science: New York, 2009.
(25) Wang, T. Y.; Fang, C. M.; Sheng, Y. J.; Tsao, H. K. Osmotic Pressure and Virial Coefficients of Star and Comb Polymer Solutions: Dissipative Particle Dynamics. *J. Chem. Phys.* **2009**, *130*, 124904.
(26) Lin, Y. L.; Wu, M. Z.; Sheng, Y. J.; Tsao, H. K. Effects of Molecular Architectures and Solvophobic Additives on the Aggregative Properties of Polymeric Surfactants. *J. Chem. Phys.* **2012**, *136*, 104905.
(27) Israelachvili, J.; Mitchell, J.; Ninham, B. W. Theory of Self-Assembly of Hydrocarbon Amphiphiles into Micelles and Bilayers. *J. Chem. Soc., Faraday Trans.* **1976**, *72*, 1525−1568.
(28) Hoshen, J.; Kopelman, R. Percolation and Cluster Distribution. I. Cluster Multiple Labeling Technique and Critical Concentration Algorithm. *Phys. Rev. B* **1976**, *14*, 3438−3445.